



## Research Paper

## Direct catalytic conversion of carbohydrates to methyl levulinate: Synergy of solid Brønsted acid and Lewis acid



Lingyun Jiang<sup>a</sup>, Lipeng Zhou<sup>a</sup>, Jinyu Chao<sup>a</sup>, Huiting Zhao<sup>a</sup>, Tianliang Lu<sup>b</sup>, Yunlai Su<sup>a</sup>, Xiaomei Yang<sup>a,\*</sup>, Jie Xu<sup>c</sup>

<sup>a</sup> College of Chemistry and Molecular Engineering, Zhengzhou University, 100 Kexue Road, Zhengzhou 450001, China

<sup>b</sup> School of Chemical Engineering and Energy, Zhengzhou University, 100 Kexue Road, Zhengzhou 450001, China

<sup>c</sup> State Key Laboratory of Catalysis, Dalian National Laboratory for Clean Energy, Dalian Institute of Chemical Physics, Chinese Academy of Sciences, 457 Zhongshan Road, Dalian 116023, China

## ARTICLE INFO

## Keywords:

Methyl levulinate

Glucose

Sn-Beta

Carbohydrates

## ABSTRACT

Conversion of biomass derived carbohydrates to alkyl levulinates is an important process due to the wide application of alkyl levulinates as chemicals and biofuel additives. Efficient conversion of cheap and abundant glucose to alkyl levulinates over easily separated and regenerated solid catalyst is highly desirable. Here, the transformation of glucose to methyl levulinate (MLE) was studied over dual solid acid catalysts. The synergistic effect of solid Brønsted (B) acid and solid Lewis (L) acid was observed. A combined catalyst system consisting of both B acid and L acid was found to be more efficient for the production of MLE from glucose. 62% yield of MLE was given over the combined catalyst of  $\text{SO}_4^{2-}/\text{ZrO}_2$  and Sn-Beta prepared by postsynthesis method at 170 °C for 24 h. The roles of L acid sites of  $\text{SO}_4^{2-}/\text{ZrO}_2$  and Sn-Beta, and B acid sites of  $\text{SO}_4^{2-}/\text{ZrO}_2$  were discussed in detail. Alternative biomass-derived carbohydrates also gave moderate to good yields of MLE. Recyclability studies indicated that the combined catalyst system can be reused without significant change in the yield of MLE, proving its easy recovery and thermal stability during regeneration.

## 1. Introduction

Utilization of renewable resources has attracted great attention in recent years due to the consumption of fossil resources and the increase of environmental problems related to using fossil resources such as coal, oil and natural gas. Biomass resources are good candidates for sustainable production of biofuels and chemicals with minimal adverse environmental effects [1]. Up to now, many important chemicals, such as ethanol, lactic acid, furfural, levulinic acid (LA) and polyol, have been produced by transformation of biomass derived carbohydrates using catalytic route [2]. LA is one kind of the most important chemicals derived from biomass, which has been identified by the United States Department of Energy to be one of the top 10 valuable platform chemicals upon which biorefining processes may be established [3]. LA can be further upgraded to alkyl levulinates through esterification of LA with various alcohols. Alkyl levulinates can be used as plasticizing materials, solvents, odor substances and fuel additives [2a,4]. They can also be converted to aminolevulinic acid, succinic acid, 1,4-diols,  $\gamma$ -valerolactone and its derivatives, and fuels [4a]. Alkyl levulinates can be produced in good yields starting from purified LA over acidic

catalysts such as  $\text{H}_2\text{SO}_4$ , heteropolyacids, Amberlyst-15, and sulphated oxides [5]. The synthesis of alkyl levulinates can also be achieved in high yields (> 90%) via decomposition of 5-hydroxymethyl furfural (HMF) or furfural alcohol in alcohol over various acidic catalysts including mineral acids (e.g. HCl and  $\text{H}_2\text{SO}_4$ ), metal salts (e.g.  $\text{AlCl}_3$  and  $\text{Al}_2(\text{SO}_4)_3$ ) and solid acids (e.g. HBeta, HZSM-5,  $\text{SO}_4^{2-}/\text{ZrO}_2$ - $\text{TiO}_2$  and  $\text{H}_3\text{PW}_{12}\text{O}_{40}/\text{ZrO}_2$ -Si(Ph)Si) [6]. However, the cost of HMF or furfural alcohol is relatively high. Moreover, HMF and furfural alcohol are mainly produced using carbohydrates as raw materials. From a processing viewpoint, using HMF or furfural alcohol as reactant is complicated and uneconomic. Direct conversion of carbohydrates to alkyl levulinates without separating intermediate such as LA or HMF from reaction mixture is more attractive. Therefore, development of highly efficient catalytic system for one-pot conversion of carbohydrates into alkyl levulinates would be desirable.

Brønsted (B) acid catalysts are effective for the transformation of fructose to alkyl levulinates directly with alcohol as both solvent and reactant.  $\text{SO}_3\text{H}$ -SBA-15 gave 58% yield of methyl levulinate (MLE) for the conversion of fructose [7]. 80% yield of MLE was achieved over acidic  $\text{TiO}_2$  nanoparticles [8]. Under the optimal conditions 86% yield

\* Corresponding author.

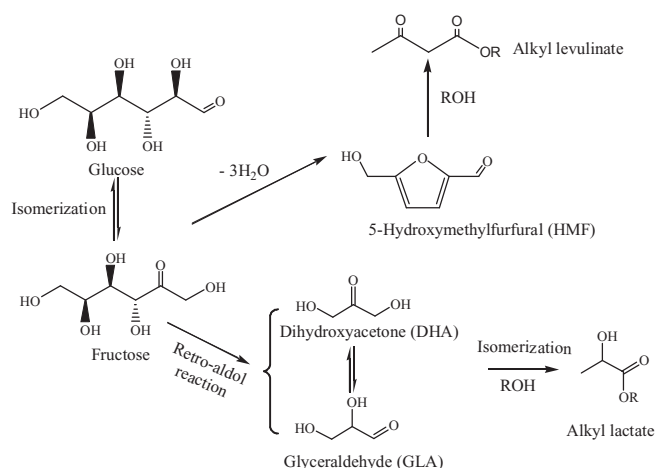
E-mail address: [yangxiaomei@zzu.edu.cn](mailto:yangxiaomei@zzu.edu.cn) (X. Yang).

<http://dx.doi.org/10.1016/j.apcatb.2017.08.072>

Received 12 March 2017; Received in revised form 20 July 2017; Accepted 21 August 2017

Available online 25 August 2017

0926-3373/ © 2017 Elsevier B.V. All rights reserved.



Scheme 1. Proposed reaction pathway for the conversion of glucose.

of ethyl levulinate was given over sulfonic acid-functionalized carbon materials [9]. Fructose is less abundant and more expensive than glucose. Unfortunately, for the conversion of glucose to LA and its esters, B acid is not as effective as for the conversion of fructose [10]. Direct conversion of glucose to alkyl levulinates is more complex and difficult than fructose, which involves the isomerization of glucose to fructose, dehydration of fructose to HMF, and alcoholysis of HMF to levulinate esters (Scheme 1) [11]. In general, B acid is more efficient than Lewis (L) acid for the dehydration of carbohydrates and alcoholysis of HMF. L acid catalysts show higher catalytic activity for the isomerization of glucose to fructose as compared with B acid [12]. Therefore, the catalyst system bearing both B and L acid sites is essential for the direct conversion of glucose to alkyl levulinates.

Using the strategy of cooperation of B and L acid as catalyst was illustrated for the conversion of biomass, such as for glycerol dehydration to acrolein catalyzed by zeolite [13], for glucose conversion to HMF over mesoporous Nb-W oxides, tantalum oxide and zeolite [14], and for cellobiose conversion to HMF in water over niobium phosphate [15]. Recently, one pot conversion of glucose to HMF or 5-(ethoxymethyl)furfural catalyzed by the combination of zeolite and organic sulfonic acid resin was reported [16]. Tominaga et al. explored the B and L mixed-acid system as an efficient way to synthesize MLE [17]. Recently, it was reported that the L ( $\text{CrCl}_3$ ) and B ( $\text{H}_3\text{PO}_4$ ) acid had a strong synergistic catalytic activity for the conversion of glucose to LA [18]. Although homogenous L and B acid system is active, it still has drawbacks of difficult separation and corrosion of reactor.

Zeolites, containing both L and B acid sites, have been shown to be efficient for such conversions [19]. Recently, our group reported that mesoporous HUSY was more active than conventional HUSY, which gave 32% yield of MLE from glucose at 160 °C for 5 h [11]. However, the catalytic activity of aluminosilicate zeolites for the conversion of glucose to alkyl levulinates is still deficient due to the relatively weak acidity of these catalysts. Therefore, designing an efficient, cost-effective, easily recyclable and heterogeneous catalyst system for the conversion of glucose to alkyl levulinates is imperative.

Sn-Beta zeolite is an excellent catalyst for the isomerization of glucose to fructose. Davis and coworkers reported that 31% yield of fructose was given using Sn-Beta as catalyst at 110 °C for 30 min [20]. Therefore, combination of a solid B acid with Sn-Beta is a possible proposal for efficient conversion of glucose to alkyl levulinates. Consideration of the catalyst recycling during the conversion of sugars, a solid catalyst system with high thermal stability is more suitable so that the byproducts such as humins deposited on the catalyst can be removed by calcination in air. In the present work, a series of solid L acids (Sn-, Zr-, Ti-, Ce-Beta) combined with B acids including commercial zeolites and sulfonated materials as catalysts are investigated for the

direct conversion of glucose to MLE in a one-pot reaction protocol. It is found that strong B acid and L acid showed synergistic effect for the formation of MLE using glucose as substrate. The acid strength of B acid of the combined catalyst system greatly determined the yield of MLE. Strong B acid is essential for the conversion of glucose to MLE.

## 2. Experimental section

### 2.1. Chemicals and materials

#### 2.1.1. Chemicals

Tetraethyl orthosilicate (TEOS, AR grade), tetraethylammonium hydroxide (TEAOH, 25 wt.% aqueous solution), glucose monohydrate, fructose, mannose, methyl- $\alpha$ -glucoside, methyl- $\beta$ -glucoside, sucrose and cellobiose were purchased from Aladdin Reagent Co., China. Methyl levulinate (> 99%, MLE) and methyl lactate (> 98%, MLA) were purchased from TCI Shanghai, China. Nitric acid (65–68%),  $\text{SnCl}_4 \cdot 5\text{H}_2\text{O}$  and methanol were of analytic grade and purchased from Tianjin Fengchuan Chemical Reagent Factory, China. The other chemicals were purchased from commercial source and were of AR grade. All chemicals were used as received without further purification.

Beta, USY, ZSM-5, MOR and Y zeolite powder were purchased from Nankai University Catalyst Co., China.  $\text{NH}_4$ -form zeolites were obtained by ion-exchanging twice with  $\text{NH}_4\text{NO}_3$  solution ( $0.5 \text{ mol L}^{-1}$ ) at 80 °C for 2 h. The protonic form was obtained by calcination of the  $\text{NH}_4$ -type zeolites at 550 °C for 5 h. HUSY-meso was prepared by treatment of USY with  $0.2 \text{ mol L}^{-1}$   $\text{HNO}_3$ . The detail procedure can be found in reference [11]. XRD patterns (Fig. S1) show these zeolites are in pure phase except for HBeta with a minor of impurity.

#### 2.1.2. Preparation of Sn-, Zr-, Ti-Beta by hydrothermal method (Sn-, Zr-, Ti-Beta-h)

The procedure for synthesis of transition metal substituted Beta by hydrothermal method was similar with that described in reference [21]. In a typical synthesis procedure for Sn-Beta-h, TEAOH was mixed with TEOS in a plastic beaker. After stirring for 90 min,  $\text{SnCl}_4$  solution was added dropwise. The mixture was heated to 60 °C to evaporate ethanol completely. Then, HF (40 wt.% aqueous solution) was added, and the dense gel was formed. Finally, the above dealuminated Beta seeds (~4 wt.%, based on the theoretical zeolite amount) were suspended in deionized water, sonicated and added into the dense gel. The molar ratio of the resulting gel was as follows:  $0.008 \text{ SnO}_2$ :  $1 \text{ SiO}_2$ :  $0.54 \text{ TEAOH}$ :  $0.54 \text{ HF}$ :  $7.5\text{H}_2\text{O}$ . After the gel was mixed homogeneously, it was transferred to a stainless steel autoclave lined with PTFE, and crystallized statically at 140 °C for 30 days. After crystallization, the autoclave was cooled down to room temperature quickly and the products were isolated by centrifugation. The products were washed three times with deionized water and dried at 100 °C overnight. The dried powder was calcined in muffle furnace at 550 °C for 8 h to remove carbonaceous residues. Zr-Beta-h was synthesized by similar procedure except for using  $\text{ZrOCl}_2 \cdot 8\text{H}_2\text{O}$  as the source of zirconium. For synthesis of Ti-Beta-h,  $\text{Ti}(\text{O}i\text{Bu})_4$  was used and  $\text{H}_2\text{O}_2$  was added to  $\text{Ti}(\text{O}i\text{Bu})_4$  with the molar ratio of  $\text{Ti}/\text{H}_2\text{O}_2$  of 0.5. The other procedure is same with that for Sn-Beta-h.

#### 2.1.3. Preparation of Sn-, Ce-Beta by postsynthesis route (Sn-, Ce-Beta-p)

The postsynthesis of Sn-Beta zeolite was carried out according to our reported procedure [22]. The parent Al-Beta zeolite was dealuminated with nitric acid ( $13 \text{ mol L}^{-1}$ ,  $20 \text{ mL g}^{-1}$  zeolite) at 100 °C for 20 h. After filtration and washing by water until the filtrate was near neutral, the dealuminated zeolite was dried at 100 °C overnight. The Si/Al molar ratio of dealuminated Beta determined by ICP-AES is 1470. The solid-state ion-exchange was performed by grinding 0.03 g of  $\text{SnCl}_4 \cdot 5\text{H}_2\text{O}$  with 0.5 g of dried dealuminated Beta for 1 h. After drying again at 100 °C overnight, the sample was calcined at 550 °C for 6 h, which was denoted as Sn-Beta-p. For synthesis of Ce-Beta-p, similar

procedure was used with  $\text{Ce}(\text{NO}_3)_3 \cdot 6\text{H}_2\text{O}$  as the source of Ce. The nominal content of Sn and Ce is 2 wt.%. It should be noted that Ti- or Zr-Beta-p synthesized via postsynthesis method using  $\text{Ti}(\text{OBU})_4$  or  $\text{ZrOCl}_2 \cdot 8\text{H}_2\text{O}$  as the source of Ti or Zr, respectively, almost has no L acidity.

#### 2.1.4. Preparation of $\text{SO}_4^{2-}/\text{ZrO}_2$

$\text{ZrOCl}_2 \cdot 8\text{H}_2\text{O}$  was dissolved in de-ionized water to give a solution (20 wt.%). Concentrated  $\text{NH}_3 \cdot \text{xH}_2\text{O}$  (25 wt.%) was added into the above solution under stirring. The mixture was aged at room temperature for 24 h. The obtained precipitate was filtered and washed thoroughly with de-ionized water until no chloride ion was detected by  $\text{AgNO}_3$  solution ( $0.1 \text{ mol L}^{-1}$ ). Then it was dried at  $100^\circ\text{C}$  for 24 h. The dried precipitate was powdered below 80 meshes. The sieved powder was impregnated with a  $1.0 \text{ mol L}^{-1}$   $\text{H}_2\text{SO}_4$  solution with a solution/solid ratio of  $15 \text{ mL g}^{-1}$  and stirred at 500 rpm for 2 h. The resulting precipitated solid was filtered, subsequently dried at  $100^\circ\text{C}$  for 24 h and calcined at  $500^\circ\text{C}$  for 3 h in static air.

#### 2.2. Characterization

The synthesized catalysts were characterized by X-ray diffraction on a Panalytical X'Pert Pro diffractometer with Cu K $\alpha$  radiation. The XRD patterns of the solid samples are shown in Fig. S1. The Si/Al ratio of zeolites was determined by a Philips Margix X-ray fluorescence (XRF) spectrometer. Metal content of Me-Beta was detected by ICP. Textural properties were measured using nitrogen adsorption–desorption isotherms with a Quantachrome Autosorb. Samples were outgassed at  $300^\circ\text{C}$  for 2 h under vacuum prior to measurements. Total surface area was calculated according to Brunauer-Emmet-Taller (BET) method. Thermal analysis was performed on a NETZSCH STA 449F3 thermal analyzer under nitrogen atmosphere with a temperature ramp of  $10^\circ\text{C min}^{-1}$ . The acid strength of solid acids was estimated using Hammett organic base indicators. The indicators were dissolved in dry cyclohexane (5 wt.%). Before performing tests, the sample was removed water by heating at  $300^\circ\text{C}$  for 1 h. After cooling to ambient temperature, the sample (0.1 g) was added into 5 mL of dry cyclohexane containing two drops of indicator solution. The mixture was left for 1 h to reach equilibrium before recording changed color. Temperature-programmed desorption of ammonia ( $\text{NH}_3$ -TPD) was performed on a Micromeritics AutoChem II 2920 instrument. Before the adsorption of  $\text{NH}_3$ , the sample (0.1 g) was pretreated at  $350^\circ\text{C}$  in He ( $30 \text{ mL min}^{-1}$ ) for 30 min. Then the sample was cooled down to  $100^\circ\text{C}$  and adsorbed  $\text{NH}_3$  for 0.5 min. Subsequently, the catalyst was flushed with He until the baseline was steady. The desorption process was monitored with a thermal conductivity detector at a temperature ramp from 100 to  $800^\circ\text{C}$ , with a heating rate of  $10^\circ\text{C min}^{-1}$ . Fourier transform infrared (FT-IR) spectra of pyridine and  $\text{CD}_3\text{CN}$  adsorption were recorded on self-supporting wafers ( $\sim 13 \text{ mg}$ ). After evacuated at  $450^\circ\text{C}$  for 3 h, the wafers were cooled down to room temperature and the spectrum of hydroxyl region was acquired as the background spectrum. Subsequently, pyridine or  $\text{CD}_3\text{CN}$  was adsorbed until saturation. For pyridine-IR, the temperature was raised to the desired value and kept for 0.5 h. The spectrum was collected after the temperature was decreased again to room temperature. For  $\text{CD}_3\text{CN}$ -IR, the spectrum was collected at room temperature with different desorption time.

#### 2.3. Reaction procedure and product analysis

The performance of the catalysts was studied in a high pressure 80 mL batch stirred reactor with a Teflon liner. The liner was first loaded with methanol, and then a certain amount of carbohydrate and catalyst was added. After the autoclave was sealed, the atmosphere over the solution was flushed with  $\text{N}_2$  four times, and then the pressure of  $\text{N}_2$  was charged to 0.4 MPa initially. Subsequently, the reactor was heated

to the desired temperature at a heating rate of  $5^\circ\text{C min}^{-1}$  under the stirring speed of 600 rpm. When the reaction was finished, the reactor was cooled down to the ambient temperature in water bath. The products in the reaction mixture were identified by an Agilent 6890N GC/5973 MS. Standard reference compounds were used for identification by GC and HPLC analysis. Conversion of glucose and yields of fructose, mannose and methyl glucoside were analyzed with the external standard method on a Shimadzu LC-20AT HPLC analysis system equipped with an Aminex HPX-87H column ( $300 \text{ mm} \times 7.8 \text{ mm}$ ) and refractive index detector (RID-10A).  $\text{H}_2\text{SO}_4$  ( $0.005 \text{ mol L}^{-1}$ ) was used as the mobile phase under the column temperature of  $40^\circ\text{C}$ , which had a flow rate of  $0.5 \text{ mL min}^{-1}$ . Yields of MLE and MLA were analyzed on a GC equipped with an FID detector using naphthalene as the internal standard.

### 3. Results and discussion

#### 3.1. Screening of acid catalysts for the conversion of glucose

The acidity of the tested catalysts was characterized first by  $\text{NH}_3$ -TPD (Fig. S2) and pyridine-IR (Fig. S3) due to the pivotal role of acidity in the conversion of glucose to MLE. The acid amount calculated based on the  $\text{NH}_3$ -TPD and the ratio of  $n_L/n_B$  were listed in Table S1. Transition metal substituted Beta zeolites synthesized by the hydrothermal method (Sn-, Zr-, Ti-Beta-h) only have L acid sites derived from the framework heteroatom [23], which was proved by pyridine-IR (Fig. S3). Although the theoretical content of the metals is identical, the acid amount decreased in the order of Zr-Beta-h > Sn-Beta-h > Ti-Beta-h. The L acid density of Zr-Beta-h and Sn-Beta-h is close to their metal content. The L acid density of Ti-Beta-h is lower than the titanium content, implying that incorporation of Ti into the framework of Beta is difficult. For Me-Beta synthesized by the postsynthesis method (Sn- and Ce-Beta-p), a large amount of L acid sites with a few of B acid sites ( $n_L/n_B = 4.22\text{--}14.9$ ) was found. The small amount of B acid sites originates from the trace amount of residual framework Al (0.03 wt.%). The L acid density of Ce-Beta-p is about half to its metal content, indicating partial cerium was incorporated into the framework. Aluminosilicate zeolites ( $n_L/n_B = 0.35\text{--}1.40$ ) and  $\text{SO}_4^{2-}/\text{ZrO}_2$  ( $n_L/n_B = 1.16$ ) have both L and B acid sites. However, the B acid strength of  $\text{SO}_4^{2-}/\text{ZrO}_2$  is much higher than aluminosilicate zeolites and it was accordant with the results of the titration with Hammett method (Table S2). IR peaks at  $1450\text{--}1454 \text{ cm}^{-1}$  of pyridine adsorbed on aluminosilicate zeolites are attributed to pyridine interacting with L acid sites. For  $\text{SO}_4^{2-}/\text{ZrO}_2$ , the band shifts to  $1447 \text{ cm}^{-1}$  which is close to hydrogen bonded pyridine [24]. The red shift of the band maybe attribute to the weaker L acid strength of  $\text{SO}_4^{2-}/\text{ZrO}_2$  than aluminosilicate zeolites. For aluminosilicate zeolites, the B acid density is lower than the content of aluminum, implying extraframework aluminum species exist in these samples [25]. Commercial acidic ion-exchange resin Amberlyst-15 is a typical B acid ( $c_{\text{H}^+} = 4.7 \text{ mmol g}^{-1}$ ).

To reveal the roles of L and B acid sites in the conversion of glucose in methanol, different solid acid samples were first screened (Table 1). In blank experiment (entry 1), only trace amount of MLA (2% yield) formed at  $160^\circ\text{C}$  for 5 h. Solid L acid catalysts, including Sn-Beta-h, Ti-Beta-h, Zr-Beta-h, Sn-Beta-p and Ce-Beta-p (entries 2–6) gave MLA as the main product. The highest yield of MLA (43%) was obtained over Sn-Beta-h prepared by the hydrothermal route. Amberlyst-15, a pure B acid catalyst, gave 24% yield of MLE without formation of MLA (entry 7). Additionally, Amberlyst-15 showed much higher catalytic activity for the formation of MLE from fructose (75% yield).  $\text{SO}_4^{2-}/\text{ZrO}_2$  gave similar product distribution with Amberlyst-15 (entry 9) and the yield of MLE (18%) is still not satisfying. Aluminosilicate zeolites including HY, HMOR, HZSM-5, HBeta, HUSY and HUSY-meso gave MLE as the main product with minor MLA as a by-product (entries 10–15). The highest yield of MLE (38%) was obtained using mesoporous HUSY as catalyst.

**Table 1**  
Screening acid catalyst for glucose conversion.<sup>a</sup>

Entry	Catalyst	Conversion (%)	Product yield (%)	
			MLE	MLA
1	Blank	50	~0	2
2	Sn-Beta-h	> 99	~0	43
3	Ti-Beta-h	99	~0	37
4	Zr-Beta-h	> 99	~0	32
5	Sn-Beta-p	98	4	18
6	Ce-Beta-p	95	2	11
7	Amberlyst-15	93	24	~0
8 <sup>b</sup>	Amberlyst-15	> 99	75	~0
9	SO <sub>4</sub> <sup>2-</sup> /ZrO <sub>2</sub>	> 99	18	~0
10	HY	> 99	35	~0
11	HMOR	90	5	~0
12	HBeta	> 99	18	~0
13	HZSM-5	> 99	2	3
14	HUSY	> 99	31	4
15	HUSY-meso	> 99	38	2

<sup>a</sup> Reaction conditions: glucose (0.374 g), catalyst (0.20 g), methanol (12.0 g), 0.4 MPa N<sub>2</sub>, 160 °C, 5 h. MLE = methyl levulinate, MLA = methyl lactate.

<sup>b</sup> Fructose as substrate.

The formation of MLA from glucose comprises isomerization of aldose to ketose, retro-aldol reaction to trioses, and isomerization of trioses to alkyl lactate [26]. These steps mainly catalyzed by L acid sites [27]. Sn-Beta-h showed much higher yield of MLA than Sn-Beta-p (Table 1), although their acidity has no obvious difference (Table S1). It is reported that Me-Beta-h prepared in fluoride media by the hydrothermal method has few defects and the surface is hydrophobic [20]. Me-Beta-p prepared by the postsynthesis method has plenty of Si-OH defects. The defects on Me-Beta-p retard the retro-aldol reaction of fructose to C<sub>3</sub> compounds, resulting in the low yield of MLA [22].

When pure B acid was used as catalyst, MLE was the main product without formation of MLA (Table 1, entry 7). It is widely accepted that B acid is active for the dehydration reaction [28]. Usually, the conversion of glucose to MLE mainly contains the isomerization of glucose to fructose and the dehydration of fructose. B acid is more active than L acid for the dehydration reaction, while L acid is more active for the isomerization between aldose and ketose and the retro-aldol reaction to trioses. Therefore, low yield of MLA was formed over B acid catalyst. Aluminosilicate zeolites and SO<sub>4</sub><sup>2-</sup>/ZrO<sub>2</sub> have both L and B acid sites. As discussed above, the B acid strength of SO<sub>4</sub><sup>2-</sup>/ZrO<sub>2</sub> is stronger than that of aluminosilicate zeolites; however, aluminosilicate zeolites have moderate L acid sites [29], while the L acidity of SO<sub>4</sub><sup>2-</sup>/ZrO<sub>2</sub> is weak. L acid plays a vital role in the isomerization of glucose to fructose. The isomerization of glucose over SO<sub>4</sub><sup>2-</sup>/ZrO<sub>2</sub> and HUSY-meso was done at 100 °C for 1 h (Table S3). The fructose yield over HUSY-meso was 47%, implying that glucose could be smoothly isomerized to fructose over the catalyst. No fructose was observed over SO<sub>4</sub><sup>2-</sup>/ZrO<sub>2</sub>, and only a certain amount of methyl glucoside (15% yield) was given. It indicates that SO<sub>4</sub><sup>2-</sup>/ZrO<sub>2</sub> showed poor activity for the isomerization of glucose to fructose in methanol. Therefore, HUSY-meso gave much higher yield of MLE than SO<sub>4</sub><sup>2-</sup>/ZrO<sub>2</sub>.

### 3.2. Catalytic conversion of glucose over B acid combined with L acid

As mentioned above, Amberlyst-15, commercial zeolites and SO<sub>4</sub><sup>2-</sup>/ZrO<sub>2</sub> gave low or moderate MLE yield from glucose in methanol. L acid catalyst was found to be selective for MLA formation in the conversion of glucose in methanol. In the following study, the conversion of glucose to MLE was examined over a B acid combined with an L acid as catalyst. When Amberlyst-15, a pure B acid, combined with Sn-, Ti-, or Zr-Beta zeolite as catalyst, the yield of MLE significantly increased as compared to using Amberlyst-15 alone (Table 1, entry 7 and Table 2). Among Me-Beta-h zeolites synthesized by the hydrothermal

**Table 2**  
Conversion of glucose to MLE over Amberlyst-15 combined with Lewis acid.<sup>a</sup>

Entry	Catalyst	Conversion (%)	Y <sub>MLE</sub> (%)	Y <sub>MLA</sub> (%)
1	Amberlyst-15 + Sn-Beta-h	> 99	51	4
2	Amberlyst-15 + Ti-Beta-h	96	38	2
3	Amberlyst-15 + Zr-Beta-h	95	39	2
4	Amberlyst-15 + Sn-Beta-p	> 99	53	7
5	Amberlyst-15 + Ce-Beta-p	96	12	~0

<sup>a</sup> Reaction conditions: glucose (0.374 g), Amberlyst-15 (0.10 g), Me-Beta (0.10 g), methanol (12.0 g), 0.4 MPa N<sub>2</sub>, 160 °C, 5 h.

method, Sn-Beta-h combined with Amberlyst-15 gave the highest yield of MLE (Table 2, entry 1). Interestingly, Amberlyst-15 combined with Sn-Beta-p prepared by the postsynthesis method gave a slightly higher yield of MLE (Table 2, entry 4) than Amberlyst-15 combined with Sn-Beta-h, although low yield of MLA was obtained over Sn-Beta-p alone.

The isomerization of glucose to fructose over Me-Beta zeolites was carried out in methanol at 100 °C to reveal the activity difference between these Me-Beta zeolites (Table S3). It can be seen that the yields of fructose and its derivatives decreased in the order of Sn-Beta-p (61%) > Sn-Beta-h (42%) > Zr-Beta-h (16%) > Ti-Beta-h (11%) > Ce-Beta-p (8%), which is consistent with the order of MLE yield over L acid combined with SO<sub>4</sub><sup>2-</sup>/ZrO<sub>2</sub>. To compare the isomerization ability between Sn-Beta-p and Sn-Beta-h in detail, the conversion of glucose over the two catalysts in methanol was done at 80 °C for 1 h 40% and 26% yield of the total of fructose and its derivatives was given over Sn-Beta-p and Sn-Beta-h, respectively. Using water as solvent, 49% and 30% yield of fructose was given over Sn-Beta-p and Sn-Beta-h at 120 °C (oil bath temperature) for 2 h, respectively (Table S4). Sn-Beta-p prepared by the postsynthesis method has more Si-OH defects and weak B acidity (Fig. S3) which are favorable for the isomerization of glucose to fructose; similar phenomena were reported in the isomerization of 1,3-dihydroxyacetone to MLA catalyzed by Sn-USY [30]. Bell and coworkers calculated the isomerization of glucose to fructose over Sn-Beta catalyst and found that open Sn sites (partially hydrolyzed Sn site, ≡(Si-O)<sub>3</sub>Sn-OH) showed higher catalytic activity than closed Sn sites (fully coordinated Sn sites, ≡(Si-O)<sub>3</sub>Sn-OSi-) due to the formation of the extra flexibility provided by the defects in the lattice of open Sn sites [31]. From CD<sub>3</sub>CN-IR of Sn-Beta-p and Sn-Beta-h (Fig. S4), it can be seen that Sn-Beta-p has more open Sn sites than Sn-Beta-h. The ratio of the open sites to the total L acid sites is 0.65 and 0.46 for Sn-Beta-p and Sn-Beta-h, respectively (Table S5). So, higher activity for the isomerization of glucose was observed over Sn-Beta-p than Sn-Beta-h. For the generation of MLE from glucose, the main role of L acid is isomerizing glucose to fructose and B acid catalyzes the following step of decomposition of fructose to MLE. On the other hand, L acid can also catalyze the retro-aldol reaction of fructose to form MLA, which competes with the dehydration of fructose catalyzed by B acid. Sn-Beta-p showed the highest catalytic activity for the isomerization of glucose (Table S3) and at the same time the retro-aldol reaction of fructose to C<sub>3</sub> compound over Sn-Beta-p was limited (Table 1, entry 5), both of which account for the highest yield of MLE over Sn-Beta-p combined with Amberlyst-15 as catalyst. These results imply that a material with high activity for glucose isomerization is essential for the cascade reaction of glucose to MLE [32].

Additionally, the synthesis of Sn-Beta-p is much easier, which does not need long time for hydrothermal crystallization as compared to Sn-Beta-h [33]. Sn-Beta-p as an L acid component is suitable for the conversion of glucose to MLE, so it was fixed as the L acid component in the following study.

Sn-Beta-p (an L acid catalyst) combined with aluminosilicate zeolites or SO<sub>4</sub><sup>2-</sup>/ZrO<sub>2</sub> as B acid was studied for the conversion of glucose (Table 3). The yield of MLE over Sn-Beta-p combined with aluminosilicate zeolite is similar with aluminosilicate zeolite alone as catalyst, while the yield of MLA all increased, indicating that almost no synergy



**Table 3**

Conversion of glucose over Sn-Beta-p combined with  $\text{SO}_4^{2-}/\text{ZrO}_2$ ,  $\text{SO}_4^{2-}/\text{TiO}_2$  and zeolite.<sup>a</sup>

Catalyst	Conversion (%)	$Y_{\text{MLE}}$ (%)	$Y_{\text{MLA}}$ (%)
Sn-Beta-p + HZSM-5	> 99	7	17
Sn-Beta-p + HMOR	> 99	8	17
Sn-Beta-p + HBeta	> 99	25	12
Sn-Beta-p + HY	> 99	23	7
Sn-Beta-p + HUSY	> 99	26	11
Sn-Beta-p + HUSY-meso	> 99	24	13
Sn-Beta-p + $\text{SO}_4^{2-}/\text{ZrO}_2$	> 99	49	6
Sn-Beta-p + $\text{SO}_4^{2-}/\text{ZrO}_2^b$	> 99	46	3

<sup>a</sup> Reaction conditions: glucose (0.374 g), Sn-Beta-p (0.10 g),  $\text{SO}_4^{2-}/\text{ZrO}_2$  or zeolite (0.10 g), methanol (12.0 g), 0.4 MPa  $\text{N}_2$ , 160 °C, 5 h.

<sup>b</sup> 0.748 g of glucose was added, all of the other conditions are same.

happens between Sn-Beta-p and aluminosilicate zeolite. The yield of MLE over Sn-Beta-p combined with  $\text{SO}_4^{2-}/\text{ZrO}_2$  is 49%, which is comparable with Amberlyst-15 combined Sn-Beta-p as catalyst. When increasing the glucose amount from 0.374 g (3.1 wt.% in methanol) to 0.748 g (6.2 wt.% in methanol), comparable MLE yield was obtained (46%), showing that the catalyst still remained active at higher concentration of glucose. The strength of these B acids was examined by Hammett indicators (Table S2) [34]. The results show that  $\text{pK}_a$  of Amberlyst-15 and  $\text{SO}_4^{2-}/\text{ZrO}_2$  is higher than  $-11.4$ , which can protonate 4-nitrotoluene. The  $\text{pK}_a$  of aluminosilicate zeolites is lower than  $-8.2$ , which cannot protonate anthraquinone. These values are in agreement with those reported in literature [34]. From the above results, it can be concluded that only strong B acids, such as Amberlyst-15 and  $\text{SO}_4^{2-}/\text{ZrO}_2$ , show excellently synergistic effect with Sn-Beta-p for the conversion of glucose to MLE. There has almost no synergy between weak B acid and Sn-Beta-p. Considering the facile recyclability,  $\text{SO}_4^{2-}/\text{ZrO}_2$  was selected as the B acid component in the following study.

### 3.3. Reaction pathway over L acid combined with strong B acid

A time-course study was further conducted at 160 °C with Sn-Beta-p,  $\text{SO}_4^{2-}/\text{ZrO}_2$ , and Sn-Beta-p combined with  $\text{SO}_4^{2-}/\text{ZrO}_2$  as catalyst, respectively, to examine the reaction pathway of glucose to MLE (Fig. 1). Fig. 1a shows the results over Sn-Beta-p. Glucose was rapidly converted to fructose in the temperature-ramping process (about 30 min), and then fructose was converted mainly to MLA. After a reaction time for 150 min, only a small amount of MLE (< 3%) was generated. The concentration of methyl glucoside was low, indicating that methyl glucoside was difficult to be generated over L acid sites [35]. Fig. 1b indicates the time course of the conversion of glucose over  $\text{SO}_4^{2-}/\text{ZrO}_2$ . It can be seen that methyl glucoside (methyl- $\alpha$ -glucoside and methyl- $\beta$ -glucoside) was generated fast while MLE was formed slowly. The concentration of methyl glucoside increased with prolonging reaction time initially and decreased after 90 min. It was reported that the main product for the isomerization of glucose over  $\text{SO}_4^{2-}/\text{ZrO}_2$  in water was fructose [36]. The authors proposed that base sites ( $\text{O}^{2-}$  sites) on the surface of  $\text{ZrO}_2$  catalyzed the isomerization of glucose to fructose. In our case, fructose was not obtained due to the different reaction mechanism with water and methanol as solvent [37]. HMF was also not detected in the process of reaction. Recently, Sels and coworkers reported similar reaction pathway for the conversion of carbohydrates in alcohol media catalyzed by sulfonated polymer; no fructose or HMF was observed in the formation of MLE [38]. Fig. 1c displays the results using Sn-Beta-p combined with  $\text{SO}_4^{2-}/\text{ZrO}_2$  as catalyst. Three competing reaction pathways of glucose conversion to fructose, mannose or methyl glucoside coexist; however, the isomerization of glucose to fructose over L acid of Sn-Beta-p is faster than the two others. Therefore, the concentration of fructose at the initial stage is higher than that of methyl glucoside and mannose. With the lapse of time, fructose is rapidly transformed to other products, whereas

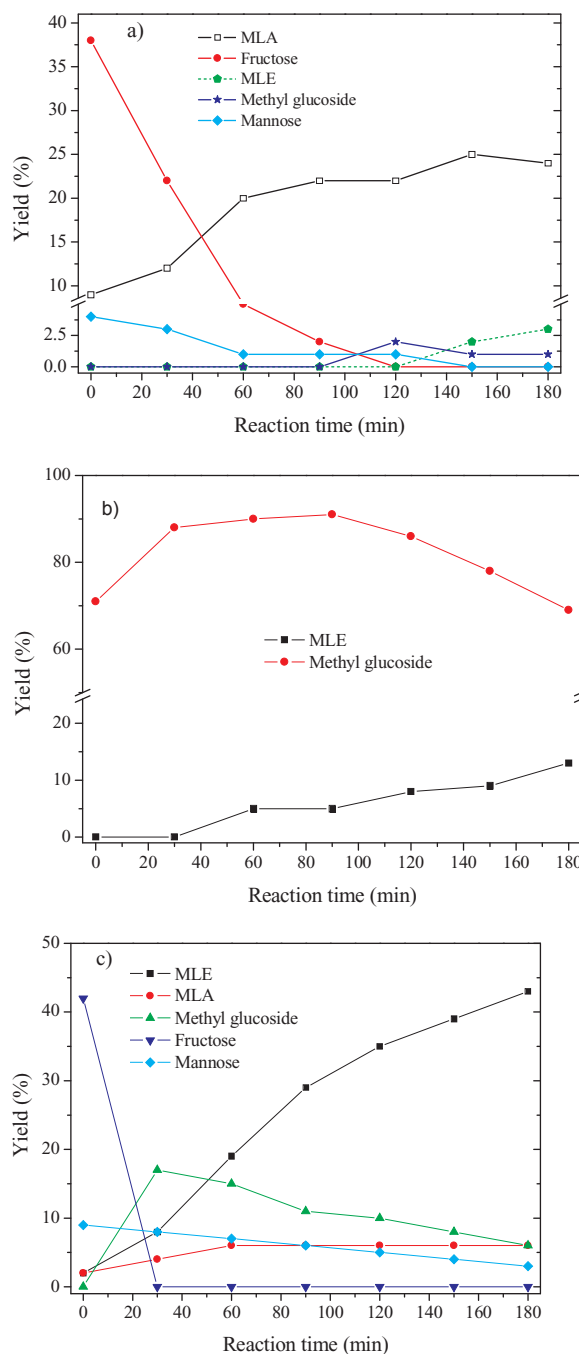
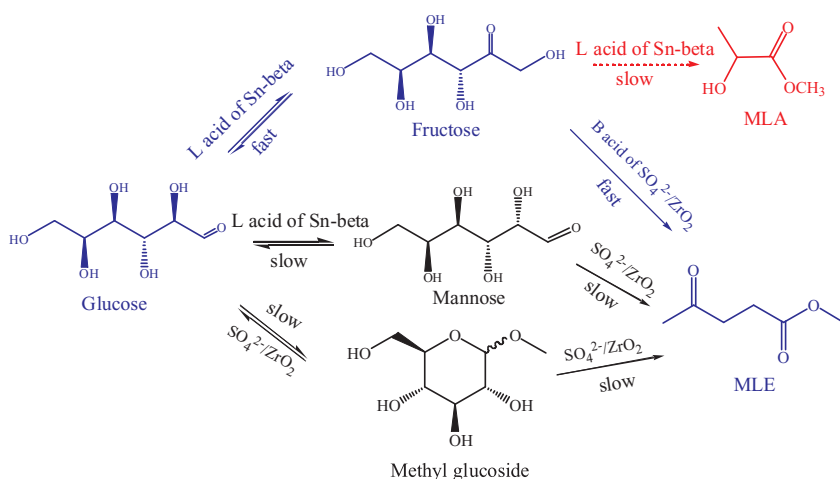


**Fig. 1.** Conversion of glucose (0.374 g) in methanol (12.0 g) at 160 °C over a) Sn-Beta-p (0.20 g), b)  $\text{SO}_4^{2-}/\text{ZrO}_2$  (0.20 g), c) Sn-Beta-p (0.10 g) combined with  $\text{SO}_4^{2-}/\text{ZrO}_2$  (0.10 g).

the conversion of mannose is slow. The yield of methyl glucoside increased quickly at the initial 30 min and then decreased slowly with the increase of time. Ultimately, mannose and methyl glucoside were converted to MLE slowly. Thus, the yield of MLE increased gradually in the whole investigated process.

The average of reaction rate related to the formation of MLE or MLA over Sn-Beta-p and  $\text{SO}_4^{2-}/\text{ZrO}_2$  is shown in Table S6. Based on the obtained results, the possible reaction pathways for the catalytic conversion of glucose are proposed in Scheme 2. Initially, glucose was rapidly converted to fructose over L acid sites of Sn-Beta-p. The reaction rate is faster than the formation of methyl glucoside catalyzed by strong B acid sites of  $\text{SO}_4^{2-}/\text{ZrO}_2$  or the epimerization of glucose to mannose over L acid sites of Sn-Beta-p. Although both mannose and methyl



**Scheme 2.** The suggested reaction pathway for the conversion of glucose to MLE over SO<sub>4</sub><sup>2-</sup>/ZrO<sub>2</sub> combined with Sn-Beta.

glucoside can also be converted to MLE, the reaction rates are much slower than the path via fructose. There are two competing reaction paths for fructose conversion. One is that fructose was dehydrated to HMF which was further decomposed to MLE over B acid sites. The other is that fructose was converted to MLA via retro-aldol reaction catalyzed by L acid sites. When strong B acid was present, the dehydration of fructose to HMF was greatly enhanced and thus MLE was the main product. To further prove the idea, the conversion of fructose over Sn-Beta-p and SO<sub>4</sub><sup>2-</sup>/ZrO<sub>2</sub> was carried out. The main product over Sn-Beta-p combined SO<sub>4</sub><sup>2-</sup>/ZrO<sub>2</sub> catalyst is MLE ( $n_{\text{MLE}}/n_{\text{MLA}} = 15$ ); without B acid (SO<sub>4</sub><sup>2-</sup>/ZrO<sub>2</sub>), the ratio of  $n_{\text{MLE}}/n_{\text{MLA}}$  decreased to 0.22. So, a strong B acid combined with a proper L acid is suitable for the efficient conversion of glucose to MLE. From the analysis of the change trend of intermediates, it can be drawn that: (1) glucose was rapidly isomerized to fructose at the initial stage over L sites of Sn-Beta-p, (2) the L sites of SO<sub>4</sub><sup>2-</sup>/ZrO<sub>2</sub> almost did not contribute to the formation of MLE, (3) no or low concentration of intermediate HMF was detected in the reaction process, implying HMF was rapidly decomposed to MLE in methanol. So, it can be concluded that the dehydration of fructose to HMF is the rate determining step for the formation of MLE from glucose, which is in accordance with literature [39].

To give additional proof on the reaction pathway for the conversion of glucose to MLE catalyzed by strong solid B acid with L acid, the time-course study on Amberlyst-15 as a B acid with Sn-Beta-p, Zr-Beta-h or Ti-Beta-h as an L acid was carried out (Fig. S6). Over Amberlyst-15, and Sn-Beta-p + Amberlyst-15 (Fig. S6a and b), similar change trend of reaction product with above was observed except for the higher activity for the formation of MLE. Using Zr-Beta-h or Ti-Beta-h as an L acid combined with Amberlyst-15 as catalyst (Fig. S6c–f), similar results were given except that mannose was negligible. The distribution of methyl glucoside over Zr-Beta-h or Ti-Beta-h combined with Amberlyst-15 is higher than over Sn-Beta-p + Amberlyst-15, while the distribution of fructose showed opposite change trend. It is because the formation of methyl glucoside from glucose catalyzed by B acid sites and the isomerization of glucose to fructose catalyzed by L acid sites are competitive reactions; Sn-Beta-p showed higher activity for the isomerization of glucose than Ti-Beta-h and Zr-Beta-h. These results further proved the above suggested reaction pathway for the conversion of glucose to MLE over an L acid combined with a strong B acid.

### 3.4. Optimization of reaction conditions

Table 4 gives the effect of L/B acid ratio on the conversion of glucose to MLE. The yield of MLE increased with the ratio of L acid to B acid at initial, and reached a maximum (54%) at the ratio of 1: 4.5. Then the yield decreased with further increasing the ratio. In addition, the yield of MLA increased with increasing the ratio of L/B acid. These

**Table 4**

Effect of the ratio of Brønsted to Lewis acid on the conversion of glucose to MLE.<sup>a</sup>

Entry	SO <sub>4</sub> <sup>2-</sup> /ZrO <sub>2</sub> (g)	Sn-Beta-p (g)	$n_{\text{Brønsted}}/n_{\text{Lewis}}$ <sup>b</sup>	MLE yield (%)	MLA yield (%)
1	0.175	0.025	10.4	40	2
2	0.160	0.040	6.0	43	3
3	0.150	0.050	4.5	54	4
4	0.134	0.066	3.0	50	5
5	0.100	0.100	1.5	49	6
6	0.050	0.150	0.5	27	12

<sup>a</sup> Reaction condition: glucose (0.374 g), methanol (12.0 g), 0.4 MPa N<sub>2</sub>, 160 °C, 5 h.

<sup>b</sup> L acid amount of Sn-Beta-p and B acid amount of SO<sub>4</sub><sup>2-</sup>/ZrO<sub>2</sub> was considered as effective L and B acid sites for the reaction, respectively. The L or B acid amount of the two samples was calculated based on the total acid amount and the ratio of B/L. The total acid amount was calculated based on NH<sub>3</sub>-TPD; the ratio of B/L was obtained from pyridine-IR spectrum at desorption temperature of 150 °C.

suggest there is a balance between L and B acid to obtain the high MLE yield. Excess L acid sites promote the retro-aldol reaction to form MLA. After the glucose was converted to fructose over L acid sites of Sn-Beta-p, fructose needed to diffuse out of the micropores of Sn-Beta-p immediately and adsorbed on the B acid sites of SO<sub>4</sub><sup>2-</sup>/ZrO<sub>2</sub> for the following dehydration step. Sn-Beta-p has plenty of mesopores due to the dealumination as described in our previous work [22], so the mass transfer will be enhanced. On the other hand, higher strength of B acid sites will increase the reaction rate of fructose conversion to MLE, resulting in the decrease of the concentration of fructose in the reaction media which is also beneficial for the diffusion of fructose out of Sn-Beta-p. So, the better synergy was observed between Sn-Beta-p and SO<sub>4</sub><sup>2-</sup>/ZrO<sub>2</sub>. Weak B acid is not sufficient for the dehydration of fructose to HMF, so almost no synergy between weak B acid and Sn-Beta-p was observed.

Further, the optimization of the reaction temperature and time was carried out (Fig. S7). The yield of MLE increased with the lapse of the reaction time. 52% and 58% yield of MLE was given at 170 °C for 2.5 h and 5 h, respectively. When the reaction time was prolonged to 24 h, 62% yield of MLE was reached. It was reported that homogenous B-L acid system (CrCl<sub>3</sub>-H<sub>3</sub>PO<sub>4</sub>) gave 56% yield of LA at 170 °C for 4.5 h using glucose as substrate [18]. 48% yield of MLE was obtained over sulfated montmorillonite at 200 °C for 4 h [40]. Al<sup>3+</sup>-exchanged montmorillonite gave 60% yield of MLE at 220 °C for 6 h [41]. 35% yield of MLE was obtained over Sn-SBA-15 at 160 °C for 20 h [42]. Using mesoporous SO<sub>4</sub><sup>2-</sup>/ZrO<sub>2</sub>-TiO<sub>2</sub> as catalyst, 45% yield of MLE was obtained at 200 °C for 2 h [43]. Fang et al. reported that 67% of MLE yield was given over bifunctional zirconia-zeolite hybrid at 180 °C for 3 h under the assistance of microwave. Heating by traditional method, only 32% yield was obtained at the same conditions [44]. Our present

**Table 5**  
Conversion of sugars to MLE catalyzed by Sn-Beta-p combined with  $\text{SO}_4^{2-}/\text{ZrO}_2$ .<sup>a</sup>

Substrate	Conversion (%)	$Y_{\text{MLE}}$ (%)	$Y_{\text{MLA}}$ (%)
Fructose	> 99	59	4
Sucrose	> 99	55	3
Mannose	> 99	31	3
Methyl- $\alpha$ -glucoside	72	31	3
Cellobiose	> 99	37	4

<sup>a</sup> Reaction conditions: carbohydrates (0.374 g), methanol (12.0 g), Sn-Beta-p (0.05 g),  $\text{SO}_4^{2-}/\text{ZrO}_2$  (0.15 g), 0.4 MPa  $\text{N}_2$ , 160 °C, 5 h.

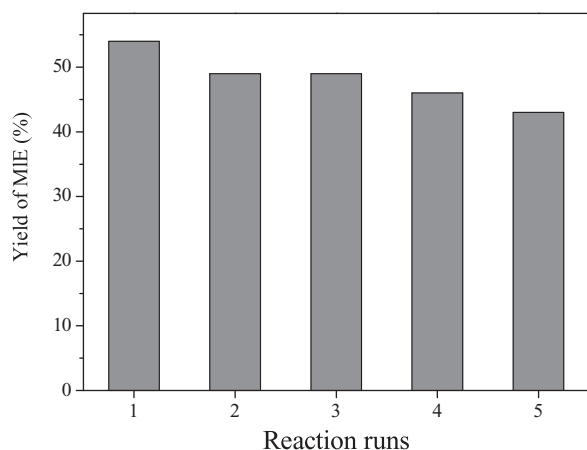


**Fig. 2.** Recycling of Sn-Beta-p combined with  $\text{SO}_4^{2-}/\text{ZrO}_2$  catalyst in the catalytic conversion of glucose to MLE. Reaction condition: glucose (0.374 g), methanol (12.0 g), Sn-Beta-p (0.05 g),  $\text{SO}_4^{2-}/\text{ZrO}_2$  (0.15 g), 0.4 MPa  $\text{N}_2$ , 160 °C, 5 h.

heterogeneous catalyst system showed superior catalytic performance than the homogenous B-L acid system and the heterogeneous catalysts reported in literature.

### 3.5. Catalytic conversion of other carbohydrates to MLE

The developed catalyst system of  $\text{SO}_4^{2-}/\text{ZrO}_2$  combined Sn-Beta-p was extended to catalyze the conversion of other carbohydrates (Table 5). Highest yield of MLE (59%) was obtained with fructose at 160 °C for 5 h. Sucrose gave similar yield of MLE with glucose. The yield of MLE is 31% from mannose and methyl- $\alpha$ -glucoside, respectively, which suggests that these intermediates can be converted to MLE slowly during the conversion of glucose. This is consistent with the results of the time course of the catalytic system in Fig. 1c. 37% yield of MLE was given from cellobiose, indicating that the catalyst is also effective for the conversion of oligosaccharides due to the high strength of B acidity of  $\text{SO}_4^{2-}/\text{ZrO}_2$  for the hydrolysis of glycosidic bonds [45].

### 3.6. Catalyst recycling in the conversion of glucose to MLE

The catalyst was evaluated for the transformation of glucose to MLE in methanol in five consecutive reaction cycles (Fig. 2). After each reaction run, the catalyst was regenerated by calcination in air at 500 °C for 3 h to remove the deposited carbonaceous products. Through all five consecutive catalytic runs, the MLE yield remained between 54% and 43%. It demonstrates the catalytic performance of the catalyst was preserved in the recycling study and suggests the catalyst system is reusable.

## 4. Conclusions

The strength of B acid and the ratio of B acid to L acid of the combined B-L acid catalyst have notable impact on the yield of MLE for the conversion of glucose. Strong B acidity and high ratio of B acid sites

to L acid sites are essential for the reaction, which restrained the formation of MLA and enhanced the yield of MLE. Sn-Beta-p as an L acid that showed good catalytic activity for the isomerization of glucose to fructose and poor catalytic activity for retro-aldol reaction gave positive contribution to improving the yield of MLE. Additionally, the L acid sites of  $\text{SO}_4^{2-}/\text{ZrO}_2$  cannot catalyze the isomerization of glucose to fructose in methanol. The combined catalyst of  $\text{SO}_4^{2-}/\text{ZrO}_2$  and Sn-Beta-p ( $n_B/n_L = 4.5$ ) was found to be an efficient catalyst system for the selective conversion of glucose to MLE, and 62% yield of MLE was obtained at 170 °C for 24 h. From the analysis of the change trend of intermediates, it can be concluded that the dehydration of fructose to HMF is the rate determining step for the formation of MLE from glucose. Recyclability studies indicated that the combined catalyst can be reused five times without significant decrease in product yield, proving its easy recovery and thermal stability during regeneration. Other biomass-derived carbohydrates also gave moderate to high yields of MLE. To further improve the yield of alkyl levulinates from biomass derived carbohydrates, an integral catalyst bearing both L acid sites and strong B acid sites was under investigation.

## Acknowledgments

We are grateful to the National Natural Science Foundation of China (21503192; J1210060), the Outstanding Young Talent Research Fund of Zhengzhou University (1521316006) and the Undergraduate Innovation Education Project of Zhengzhou University for the financial support (201610459055).

## Appendix A. Supplementary data

Supplementary data associated with this article can be found, in the online version, at <http://dx.doi.org/10.1016/j.apcatb.2017.08.072>.

## References

- [1] (a) M. Besson, P. Gallezot, C. Pinel, Chem. Rev. 114 (2014) 1827–1870; (b) R.A. Sheldon, J. Mol. Catal. A 422 (2016) 3–12; (c) L. Zhou, X. Yang, J. Xu, M. Shi, F. Wang, C. Chen, J. Xu, Green Chem. 17 (2015) 1519–1524.
- [2] (a) C. Chatterjee, F. Pong, A. Sen, Green Chem. 17 (2015) 40–71; (b) M. Stöcker, Angew. Chem. Int. Ed. 47 (2008) 9200–9211; (c) R. Zhong, F. Yu, W. Schutyser, Y. Liao, F. de Clippeel, L. Peng, B.F. Sels, Appl. Catal. B 206 (2017) 74–88.
- [3] T. Werpy, G. Petersen, A. Aden, J. Bozell, J. Holladay, A. Manheim, D. Eliot, L. Lasure, S. Jones, Top Value Added Chemicals from Biomass vol. 1, U.S. Department of Energy, Oak Ridge, TN, 2004.
- [4] (a) F.D. Pileidis, M.M. Titirici, ChemSusChem 9 (2016) 562–582; (b) P. Maki-Arvela, I.L. Simakova, T. Salmi, D.Y. Murzin, Chem. Rev. 114 (2014) 1909–1971.
- [5] (a) W. Ciptonugroho, M.G. Al-Shaal, J.B. Mensah, R. Palkovits, J. Catal. 340 (2016) 17–29; (b) X. Kong, S. Wu, X. Li, J. Liu, Energy Fuel 30 (2016) 6500–6504; (c) D. Song, S. An, Y. Sun, P. Zhang, Y. Guo, D. Zhou, ChemCatChem 8 (2016) 2037–2048; (d) M. Wu, X. Zhang, X. Su, X. Li, X. Zheng, X. Guan, P. Liu, Catal. Commun. 85 (2016) 66–69; (e) D. Unlu, O. Ilgen, N.D. Hilmioglu, Chem. Eng. J. 302 (2016) 260–268; (f) X. Zhou, Z. Li, C. Zhang, X. Gao, Y. Dai, G. Wang, J. Mol. Catal. A 417 (2016) 71–75; (g) M.A. Tejero, E. Ramirez, C. Fité, J. Tejero, F. Cunill, Appl. Catal. A 517 (2016) 56–66.
- [6] (a) Y. Huang, T. Yang, M. Zhou, H. Pan, Y. Fu, Green Chem. 18 (2016) 1516–1523; (b) M.M. Antunes, S. Lima, P. Neves, A.L. Magalhães, E. Fazio, A. Fernandes, F. Neri, C.M. Silva, S.M. Rocha, M.F. Ribeiro, M. Pillinger, A. Urakawa, A.A. Valente, J. Catal. 329 (2015) 522–537; (c) B. Lu, S. An, D. Song, F. Su, X. Yang, Y. Guo, Green Chem. 17 (2015) 1767–1778; (d) J.R. Kean, A.E. Graham, Catal. Commun. 59 (2015) 175–179.
- [7] S. Saravanamurugan, A. Riisager, Catal. Commun. 17 (2012) 71–75.
- [8] C.-H. Kuo, A.S. Poyraz, L. Jin, Y. Meng, L. Pahalagedara, S.-Y. Chen, D.A. Kriz, C. Guild, A. Gudiz, S.L. Suib, Green Chem. 16 (2014) 785–791.
- [9] R. Liu, J. Chen, X. Huang, L. Chen, L. Ma, X. Li, Green Chem. 15 (2013) 2895–2903.
- [10] A. Takagaki, M. Ohara, S. Nishimura, K. Ebitani, Chem. Commun. (2009) 6276–6278.
- [11] L. Zhou, H. Zhao, L. Cui, Y. Bai, J. Bian, T. Lu, Y. Su, X. Yang, Catal. Commun. 71

- (2015) 74–78.
- [12] (a) I. Delidovich, R. Palkovits, *ChemSusChem* 9 (2016) 547–561;  
(b) H. Nguyen, V. Nikolakis, D.G. Vlachos, *ACS Catal.* 6 (2016) 1497–1504;  
(c) J.M.R. Gallo, D.M. Alonso, M.A. Mellmer, J.A. Dumesic, *Green Chem.* 15 (2013) 85–90.
- [13] Z. Wang, L. Wang, Y. Jiang, M. Hunger, J. Huang, *ACS Catal.* 4 (2014) 1144–1147.
- [14] (a) I. Jimenez-Morales, A. Teckchandani-Ortiz, J. Santamaria-Gonzalez, P. Maireles-Torres, A. Jimenez-Lopez, *Appl. Catal. B* 144 (2014) 22–28;  
(b) I.K.M. Yu, D.C.W. Tsang, *Bioresource Technol.* 238 (2017) 716–732;  
(c) J. Guo, S. Zhu, Y. Cen, Z. Qin, J. Wang, W. Fan, *Appl. Catal. B* 200 (2017) 611–619;  
(d) M. Moreno-Recio, J. Santamaria-Gonzalez, P. Maireles-Torres, *Chem. Eng. J.* 303 (2016) 22–30;  
(e) C. Yue, G. Li, E.A. Pidko, J.J. Wiesfeld, M. Rigutto, E.J.M. Hensen, *ChemSusChem* 9 (2016) 2421–2429.
- [15] P. Carniti, A. Gervasini, F. Bossola, V. Dal Santo, *Appl. Catal. B* 193 (2016) 93–102.
- [16] (a) C.M. Lew, N. Rajabbeigi, M. Tsapatsis, *Ind. Eng. Chem. Res.* 51 (2012) 5364–5366;  
(b) T. Zhang, W. Fan, W. Li, Z. Xu, H. Xin, M. Su, Y. Lu, L. Ma, *Energy Technol.* 5 (2017) 747–755.
- [17] K. Tominaga, A. Mori, Y. Fukushima, S. Shimada, K. Sato, *Green Chem.* 13 (2011) 810–812.
- [18] (a) F. Yang, J. Fu, J. Mo, X. Lu, *Energy Fuel* 27 (2013) 6973–6978;  
(b) W. Wei, S. Wu, *Chem. Eng. J.* 307 (2017) 389–398.
- [19] (a) S. Saravanamurugan, A. Riisager, *ChemCatChem* 15 (2013) 1754–1757;  
(b) P.Y. Dapsens, C. Mondelli, J. Perez-Ramirez, *Chem. Soc. Rev.* 44 (2015) 7025–7043.
- [20] R. Bermejo-Deval, R.S. Assary, E. Nikolla, M. Moliner, Y. Román-Leshkov, S.J. Hwang, A. Palsdottir, D. Silverman, R.F. Lobo, L.A. Curtiss, *Proc. Natl. Acad. Sci. U. S. A.* 109 (2012) 9727–9732.
- [21] M.S. Holm, S. Saravanamurugan, E. Taarning, *Science* 328 (2010) 602–605.
- [22] X. Yang, J. Bian, J. Huang, W. Xin, T. Lu, C. Chen, Y. Su, L. Zhou, F. Wang, J. Xu, *Green Chem.* 19 (2017) 692–701.
- [23] H.Y. Luo, J.D. Lewis, Y. Román-Leshkov, *Annu. Rev. Chem. Biomol. Eng.* 7 (2016) 663–692.
- [24] Y. Wang, J. Ma, D. Liang, M. Zhou, F. Li, R. Li, J. Mater. Sci. 44 (2009) 6736–6740.
- [25] (a) T.D. Swif, H. Nguyen, Z. Erdman, J.S. Kruger, V. Nikolakis, D.G. Vlachos, *J. Catal.* 333 (2016) 149–161;  
(b) M. Caillot, A. Chaumonnot, M. Digne, J.A. van Bokhoven, *J. Catal.* 316 (2014) 47–56;  
(c) S.M.T. Almutairi, B. Mezari, G.A. Filonenko, P.C.M.M. Magusin, M.S. Rigutto, E.A. Pidko, E.J.M. Hensen, *ChemCatChem* 5 (2013) 452–466.
- [26] Y. Wang, W. Deng, B. Wang, Q. Zhang, X. Wan, Z. Tang, Y. Wang, C. Zhu, Z. Cao, G. Wang, H. Wan, *Nat. Commun.* 4 (2013) 2141.
- [27] (a) M. Orazov, M.E. Davis, *Proc. Natl. Acad. Sci. U. S. A.* 112 (2015) 11777–11782;  
(b) L. Zhou, L. Wu, H. Li, X. Yang, Y. Su, T. Lu, J. Xu, *J. Mol. Catal. A* 388–389 (2014) 74–79.
- [28] (a) B. Karimi, H.M. Mirzaei, H. Behzadnia, H. Vali, *ACS Appl. Mater. Interfaces* 7 (2015) 19050–19059;  
(b) D. Ding, J. Xi, J. Wang, X. Liu, G. Lu, Y. Wang, *Green Chem.* 17 (2015) 4037–4044;  
(c) F. Pepi, A. Ricci, S. Garzoli, A. Troiani, C. Salvitti, B. Di Rienzo, P. Giacomello, *Carbohydr. Res.* 413 (2015) 145–150.
- [29] Y. Chu, Z. Yu, A. Zheng, H. Fang, H. Zhang, S. Huang, S. Liu, F. Deng, *J. Phys. Chem. C* 115 (2011) 7660–7667.
- [30] X. Yang, L. Wu, Z. Wang, J. Bian, T. Lu, L. Zhou, C. Chen, J. Xu, *Catal. Sci. Technol.* 6 (2016) 1757–1763.
- [31] Y. Li, M. Head-Gordon, A.T. Bell, *ACS Catal.* 4 (2014) 1537–1545.
- [32] S. Yue, J. Sun, Y. Yi, B. Wang, F. Xu, R. Sun, *J. Mol. Catal. A* 394 (2014) 114–120.
- [33] C. Hammond, S. Conrad, I. Hermans, *Angew. Chem. Int. Ed.* 51 (2012) 11736–11739.
- [34] K. Arata, M. Hino, N. Yamagata, *Bull. Chem. Soc. Jpn.* 63 (1990) 244–246.
- [35] S. Tolborg, S. Meier, I. Sádaba, S.G. Elliot, S.K. Kristensen, S. Saravanamurugan, A. Riisager, P. Fristrup, T. Skrydstrup, E. Taarning, *Green Chem.* 18 (2016) 3360–3369.
- [36] (a) A. Osatiashtiani, A.F. Lee, D.R. Brown, J.A. Melero, G. Morales, K. Wilson, *Catal. Sci. Technol.* 4 (2014) 333–342;  
(b) A. Chareonlimkun, V. Champreda, A. Shotipruk, N. Laosiripojana, *Fuel* 89 (2010) 2873–2880.
- [37] R. Bermejo-Deval, R. Gounder, M.E. Davis, *ACS Catal.* 2 (2012) 2705–2713.
- [38] F. Yu, R. Zhong, H. Chong, M. Smet, W. Dehaen, B.F. Sels, *Green Chem.* 19 (2017) 153–163.
- [39] Z. Sun, L. Xue, S. Wang, X. Wang, J. Shi, *Green Chem.* 18 (2016) 742–752.
- [40] X. Xu, X. Zhang, W. Zou, H. Yue, G. Tian, S. Feng, *Catal. Commun.* 62 (2015) 67–70.
- [41] J. Liu, B. Yang, X. Wang, C. Liu, R. Yang, W. Dong, *Appl. Clay Sci.* 141 (2017) 118–124.
- [42] J. Pang, M. Zheng, X. Li, L. Song, R. Sun, J. Sebastian, A. Wang, J. Wang, X. Wang, T. Zhang, *ChemistrySelect* 2 (2017) 309–314.
- [43] L. Peng, J. Zhuang, L. Lin, *J. Nat. Gas Chem.* 21 (2012) 138–147.
- [44] H. Li, Z. Fang, J. Luo, S. Yang, *Appl. Catal. B* 200 (2017) 182–191.
- [45] L. Zhou, Z. Liu, Y. Bai, T. Lu, X. Yang, J. Xu, *J. Energy Chem.* 25 (2016) 141–145.